EXACT ANALYTIC SOLUTION OF THE ENVELOPE EQUATIONS FOR A MATCHED QUADRUPOLE-FOCUSED BEAM IN THE LOW SPACE CHARGE LIMIT *

O. A. Anderson, LBNL, Berkeley, CA 94720, USA
L. L. LoDestro, LLNL, Livermore, CA 94551, USA

Abstract

The Kapchinskij-Vladimirskij equations describe the evolution of the beam envelopes in a periodic system of quadrupole focusing cells and are widely used to help predict the performance of such systems. Being nonlinear, they are usually solved by numerical integration. There have been numerous papers describing approximate solutions with varying degrees of accuracy. We have found an exact solution for a matched beam in the limit of zero space charge. The model is FODO with a full occupancy, piecewise-constant focusing function. Our explicit result for the envelope $a(z)$ is exact for phase advances up to $180°$ and all other values except multiples of $180°$. The peak envelope size is minimized at $90°$. The higher stable bands require large, very accurate, field strengths while producing significantly larger envelope excursions.

INTRODUCTION

This paper treats a problem discussed by Courant and Snyder in their classic paper [1], except that we assume a straight rather than circular machine. They discussed the case in which the focus and defocus sections each had uniform focusing strength with no intervening gaps. They called this the CLS model. The model assumed negligible space charge density.

Courant and Snyder gave an explicit criterion for beam stability for the CLS model and obtained an approximate solution for the envelope. Here, we show that the CLS model is exactly solvable and explore the consequences. (Lund and Bukh [2] have given an exact analysis for the opposite case: thin lenses with maximum space-charge intensity.)

For the CLS model: (1) We find that our solutions exist in an infinite number of bands coinciding with the bands of stability. (2) We obtain a well-defined expression for phase advance σ as a function of focusing strength that applies to all bands. All values are theoretically possible except exact multiples of $180°$. (3) For fixed emittance, the peak beam radius is minimized at $\sigma = 90°$, increasing rapidly past that point. The higher bands give larger beam excursions in spite of greatly increased focusing fields [2], [3]. Although the minimum radius is reduced (cf. Ref. [4]), it is the peak radius that is significant for transport systems of fixed aperture. For such systems, in the emittance-dominated regime at least, there seems to be no advantage in increasing the focusing strength much beyond the value that gives $\sigma = 90°$.

* Work partly supported by U.S. DOE contract DE-AC02-05CH11231.

FOCUSING MODEL

We assume that the focusing strength $K(z)$ is periodic and piecewise constant with values $\pm k$ over a lattice period $2L$. This is the FD model—see Eqs. (1) and Fig. 1:

$$K(z) = +k, \qquad 0 < z < L; \tag{1a}$$
$$K(z) = -k, \qquad L < z < 2L. \tag{1b}$$

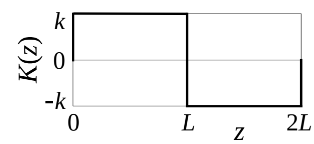

Figure 1: FD model

We assume quadrupole symmetry such that x-plane and y-plane behaviors are identical except for a shift of length L [5], [6]; we will not consider the x-plane further.

SINGLE-PARTICLE STABILITY

In the low space-charge limit, the vertical position $y(z)$ of a particle is given by

$$y''(z) + K(z)y(z) = 0, \quad K(z + 2L) = K(z). \tag{2}$$

The stability of $y(z)$ is easily found from the period-transfer matrix M [1], [7] and is given by $|\mathrm{Tr}(M)| < 2$. In the FD case this yields

$$\left|\cos\sqrt{k}L\right| < \mathrm{sech}\,\sqrt{k}L. \tag{3}$$

Figure 2 shows that there are multiple bands of real solutions over increasingly narrow ranges of $\sqrt{k}L$.

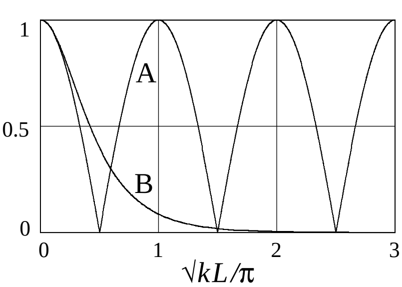

Figure 2: A = $|\cos\sqrt{k}L|$; B = $\mathrm{sech}\,\sqrt{k}L$. Stable solutions exist in the regions where curve A is below curve B.

EXACT SOLUTION OF THE ENVELOPE EQUATIONS

Without space charge, the y-plane envelope $a(z)$ of a beam with emittance ϵ is given by [7]:

$$a(z)'' + K(z)a - \frac{\in^2}{a^3} = 0. \tag{4}$$

Equation (4) could be directly integrated in terms of a^2. Instead, we use trial solutions, defining separate functions for the focus ($K > 0$) and defocus ($K < 0$) sections:

$$a(z) = \begin{cases} a_+(z) & \text{for } 0 < z < L, \\ a_-(z) & \text{for } L < z < 2L. \end{cases} \tag{5}$$

Our trial solutions utilize the symmetry of $K(z)$:

$$a_+{}^2(z) = c_+ + d_+ \cos\lambda(z - L/2), \tag{6a}$$

$$a_-{}^2(z) = c_- + d_- \cosh\lambda(z - 3L/2). \tag{6b}$$

Substitution into Eq. (4) and matching of values and derivatives of a_+ and a_- at the junctions determines the five unknown constants. This gives the matched solution

$$a_+{}^2(z) = \in L \, \frac{sn\, ch + sh \cos[\theta(2z/L - 1)]}{\mathrm{P}\,\theta\sqrt{1 - cs^2 ch^2}}, \tag{7a}$$

$$a_-{}^2(z) = \in L \, \frac{sh\, cs + sn \cosh[\theta(2z/L - 3)]}{\mathrm{P}\,\theta\sqrt{1 - cs^2 ch^2}}, \tag{7b}$$

with $\lambda = 2\sqrt{k}$ and

$$\theta \equiv \sqrt{k}L, \qquad sn \equiv \sin\theta, \qquad cs \equiv \cos\theta,$$
$$\mathrm{P} \equiv \mathrm{sign}(sn), \qquad sh \equiv \sinh\theta, \qquad ch \equiv \cosh\theta. \tag{8}$$

(The detailed derivation of Eqs. (7)—half a page—will be included in the full version of this paper.)

Figure 3 plots $a(z)/\sqrt{\in L}$ for various focusing strengths θ within the stable pass bands discussed below. Equations (7) have real solutions (pass bands) when their denominators are real. The existence criterion is

$$cs^2 ch^2 < 1. \tag{9}$$

This agrees with the stability criterion, Eq. (3), showing that a solution is stable if it exists.

PASS-BAND DETAILS

The stable bands surround the points where $\cos\theta = 0$. We call these the midpoints:

$$\theta_n \equiv (n - \tfrac{1}{2})\pi \qquad n = 1, 2, 3 \cdots \tag{10}$$

with n the pass-band number. The phase advance $\sigma(\theta)$ is given below by Eq. (14), which shows that $\cos\sigma = 0$ wherever $\cos\theta = 0$. Therefore, $\sigma_n = \theta_n$ and $\sigma_n = (n - \frac{1}{2})\pi$.

The narrow width of the pass bands beyond the first (Fig. 2) facilitates an excellent approximation for the widths when $n > 1$. For band n we write

$$\theta_{\text{edge}} = \theta_n + \delta_n. \tag{11}$$

Then, according to Eq. (3), the band edges satisfy

$$\left|\cos(\theta_n + \delta_n)\right| = \mathrm{sech}(\theta_n + \delta_n). \tag{12}$$

Taylor expansion yields

$$\theta_{\text{edge}} \simeq \theta_n \pm \frac{1}{\cosh\theta_n \pm \tanh\,\theta_n} \qquad n > 1. \tag{13}$$

For the upper edge of pass band 2, the σ_{edge} error is 10^{-5}. Eq. (13) quantifies the narrowing of the pass bands with n that is seen in Fig. 2.

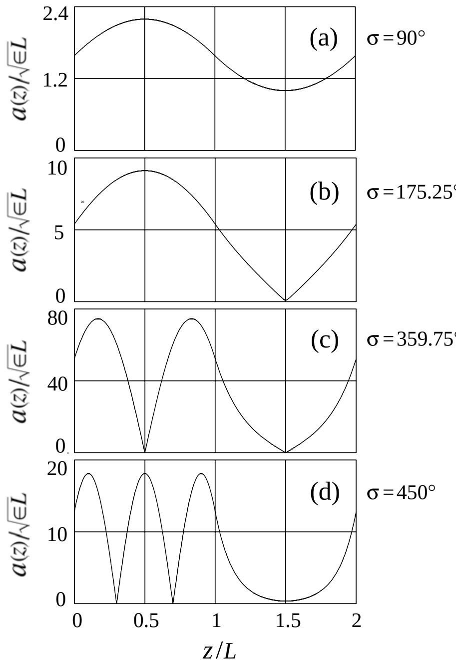

Figure 3: Plots of Eqs. (7) for various focusing strengths θ with fixed $\in$: (a) θ=0.5π, midpoint of first stable band; (b) θ=0.5968π, near band 1 edge; (c) θ=1.50561868π, near band 2 edge; (d) θ=2.5π, band 3 midpoint. Peak radius is smallest where $\sigma = \theta = 90°$ (cf. Figs. 5 and 6). Minimum envelope $a(z)$ can be very small but is always finite. In band 2, $a(z)$ and $b(z)$ have minima at the same z values; in case (c) there are huge reductions in beam area at $z = L/2$ and $3L/2$.

Full-period phase advance

From Ref. [1], the phase advance $\sigma(\theta)$ for the FD case is (assuming $|cs\, ch| < 1$),

$$\cos\sigma = \tfrac{1}{2}\,\mathrm{Tr}\,M = \cos\theta\cosh\theta, \tag{14}$$

which is ill-defined in the higher pass bands. Therefore we write

$$\Delta\theta \equiv \theta - \theta_n; \qquad \Delta\sigma \equiv \sigma - \theta_n, \tag{15}$$

where $-\frac{\pi}{2} < \Delta\sigma < \frac{\pi}{2}$ and where $\Delta\theta$ has a smaller range. Equation (14) becomes

$$\sin\Delta\sigma = \sin\Delta\theta\ \cosh\theta \tag{16}$$

with $|\sin\Delta\theta\ \cosh\theta| < 1$. Then

$$\sigma(\theta) = \theta_n + \sin^{-1}(\sin\Delta\theta\ \cosh\theta). \tag{17}$$

Here, $\sin^{-1}$ is restricted to the principal value, removing the ambiguity in Eq. 14. Figure 4 displays $\sigma(\theta)$ for the first two bands.

From Eq. (17) and Fig. 4 we see that, for any band n, σ has maximum and minimum values

$$\sigma_{\max} = n\pi, \qquad \sigma_{\min} = (n-1)\pi. \tag{18}$$

In all pass bands, σ ranges over 180°, so that arbitrary σ is possible except for the singular points $\sigma = n\pi$. The required precision of k becomes extreme near these points.

 1-4244-0917-9/07/$25.00

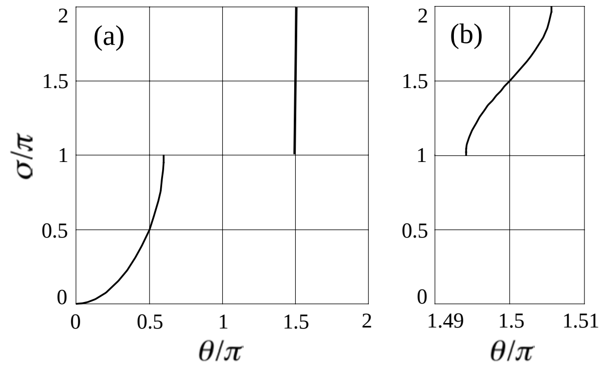

Figure 4: (a) Phase advance [Eq. (17)] for the first two stable bands. (b) Second band again with the θ axis magnified.

MAXIMUM ENVELOPE EXCURSION AND OTHER TOPICS

The peak radius $a_{\max}$ is found from Eq. (7a) by setting the cosine term (containing z) equal to P, yielding:

$$a_{+\,\max}^{2} = \in L\,\frac{\mathrm{P}\,sn\,ch + sh}{\theta\sqrt{1 - cs^2 ch^2}}. \tag{19}$$

Figure 5 illustrates Eq. (19), showing $a_{\max}/\sqrt{\in L}$ as a function of θ for the first two stable bands. In Fig. 5(a), the peak radius $a_{\max}$ decreases as the field strength increases up to the point where θ and σ reach $90°$. Further increase of θ causes a rapid increase in the peak radius, which diverges as σ approaches $180°$. In the second band, the peak radius has a minimum value where θ and σ are very close to $270°$. (Note the very small range of θ; the focusing field $\propto \theta^2$ would need to be not only very large but also accurately controlled.) The minimum peak radius in the second band is several times larger than in the first band. Thus, in the CLS model, if $\in$ and L are held constant, there is no phase advance giving a smaller peak radius than that at $90°$.

Figure 6 shows the first two bands in terms of the phase advance σ rather than the field strength parameter used for Fig. 5. Note the singular behavior at $0°$, $180°$, and $360°$.

Pass-band Midpoints

At the midpoints, the cosine factor in Eq. (7) simplifies:

$$\cos\theta\left(\frac{2z}{L} - 1\right) = \sin\left(\theta_n \frac{2z}{L}\right). \tag{20}$$

The denominators of Eqs. (7) become $\mathrm{P}\,\theta$; a^2 at the midpoint of any band n is

$$a_{+n}^{2}(z) = \in L \frac{ch_n + sh_n\,\mathrm{P}\sin(\theta_n 2z/L)}{\theta_n} \tag{21a}$$

$$a_{-n}^{2}(z) = \frac{\in L}{\theta_n}\cosh[\theta_n(2z/L - 3)]. \tag{21b}$$

Phase advance at any point

The reciprocals of Eqs. (7) can be integrated (using appropriate branch selection), yielding the exact phase advance $\sigma(z)$. [The phase advance over a full period $(0, 2L)$

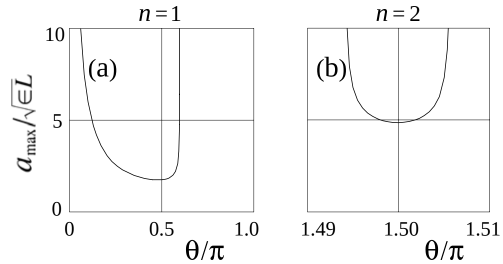

Figure 5: (a) Values of $a_{\max}/\sqrt{\in L}$ [Eq. (19)] for the first stable band. (b) The second band with the θ axis magnified. The smallest envelope excursions occur for $\theta = 90°$.

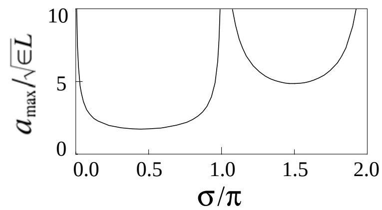

Figure 6: Values of $a_{\max}/\sqrt{\in L}$ [Eq. (19)] for the first two stable bands as a function of phase advance σ [Eq. (17)]. Minimum beam size occurs at $\sigma = 90°$.

agrees with Eq. (17), as it should.] The full version of this paper will show interesting plots of $\sigma(z)$.

Beam Matching Equation

Equation (7a) with a given $z = \text{const} \equiv \zeta$ becomes $a_\zeta = \mathrm{F}(\in, L, \zeta; \theta)$. If we choose $\zeta = 0$ and specify $\in$ and L, we can write $a_0 = \mathrm{F}(\theta)$ as the explicit condition for a matched beam. In the limit $\theta \to 0$, we find $a_0^2 \to 2\sqrt{3}\in L/\theta^2$, the usual smooth-approximation matching condition.

From another viewpoint, we observe that Eq. (4) along with periodicity of $a(z)$ constitutes a (nonlinear) eigenvalue problem and that $a_\zeta = \mathrm{F}(\in, L, \zeta; \theta)$ is the nonlinear eigenvalue equation for eigenvalue θ. This will be discussed in the full version of this paper.

ACKNOWLEDGEMENTS

We thank Ed Lee for helpful suggestions and Steve Lund for his many comments and his help with the editing.

REFERENCES

[1] E. D. Courant and H. S. Snyder, Ann. of Phys. **3**, 1 (1958).
[2] S. M. Lund and B. Bukh, Phys. Rev. ST-AB **7**, 024801 (2004).
[3] E. Lee and R. J. Briggs, Tech. Rep. LBNL-40774, UC 419, Lawrence Berkeley National Laboratory (1997).
[4] R. Pakter and F. B. Rizzato, Phys. Rev. E **65**, 056503 (2002).
[5] E. P. Lee, Phys. Plasmas **9**, 4301 (2002).
[6] O. A. Anderson, Phys. Rev. ST-AB **10**(3), 034202 (2007).
[7] H. Wiedemann, *Particle Accelerator Physics* (Springer-Verlag, New York, 1993).

